

# Optimization and variational principles for the shear strength reduction method

Stanislav Sysala<sup>1\*</sup>, Eva Hrubešová<sup>2,1</sup>, Zdeněk Michalec<sup>1</sup>

<sup>1</sup>Institute of Geonics of the Czech Academy of Sciences, Ostrava, Czech Republic

<sup>2</sup>VŠB - Technical University of Ostrava, Faculty of Civil Engineering, Ostrava, Czech Republic

February 28, 2025

## Abstract

This paper is focused on a rigorous variant of the shear strength reduction method (SSR) and the corresponding determination of safety factors. The SSR-based safety factor is defined as a solution of an optimization problem that is independent of the plastic flow rule and the space discretization. In case of nonassociative plasticity, a modified Davis approach is used. The optimization problem is analyzed and the corresponding duality between the static and kinematic principles is derived. For numerical solution, a regularization method is introduced and a relation between the original and regularized problems is derived. The regularization method is combined with the finite element method, mesh adaptivity and a damped Newton method. In-house codes in Matlab are used for implementation of this solution concept. Two slope stability problems are considered, one of which follows from analysis of a real slope. Softwares Plaxis and Comsol Multiphysics are used for comparison of the results.

**Keywords:** slope stability, shear strength reduction method, convex optimization, static and kinematic principles, regularization, finite elements and mesh adaptivity

---

\*corresponding author, email: stanislav.sysala@ugn.cas.cz

# 1 Introduction

This paper deals with slope stability assessment, which includes determination of the factor of safety (FoS) and estimation of failure zones (slip surfaces) for a critical state of the slope. Limit equilibrium (LE), shear strength reduction (SSR) or limit analysis (LA) belong among basic methods that can be used for the determination of FoS. The methods arise from elastic-perfectly plastic models containing mainly the Mohr-Coulomb yield criterion.

The LE method is based on predefined failure zones, see, for example, [Duncan (1996)], [Yu (2006)]. It does not require finite element computation and stresses equilibrium at every point in a domain around the slope. Due to these facts, this method is simple and widely used in geotechnical practice. On the other hand, accuracy of the solution cannot be easily verified, especially if anisotropic or inhomogeneous materials are considered or if a complex geometry is defined.

The SSR method [Zienkiewicz et al. (1975), Brinkgreve and Bakker (1991)], [Dawson et al. (1999), Griffiths and Lane (1999)] has been suggested mainly for the slope stability assessment. It is a conventional method based on a displacement variant of the finite element method (FEM) and on reduction of strength parameters defining the Mohr-Coulomb model. It has also been implemented within some commercial softwares like Plaxis [Brinkgreve (2011)] or Middas GTS NX. Strong dependence on finite element mesh density or even nonunique determination of FoS can happen in some cases with the non-associative plastic flow rule, see [Tschuchnigg et al. (2015a), Tschuchnigg et al. (2015b)].

LA is a universal method that can be used for various stability problems, not only for the ones in geotechnical practice. FoS is derived from a critical (limit) value of the load factor. Originally, this method was purely analytical, see, for example, [Chen and Liu (1990)]. Now, it is rather a numerical method based on optimization, duality between kinematic and static principles and on FEM [Christiansen (1990), Sloan (2013), Yu (2006), Haslinger et al. (2019)]. LA is supported by mathematical and numerical analyses, see [Temam (1985), Christiansen (1990), Haslinger et al. (2016a), Repin et al. (2018)], [Haslinger et al. (2019)]. On the other hand, this method is not so conventional in slope stability and may predict different FoS than the SSR or LE methods. The theory of LA method is not also fully developed for the non-associative plastic flow.

The usage of the non-associative plastic flow rule is supported by laboratory experiments in order to catch volume dilatancy of materials with internal friction. On the other hand, mathematical theory of non-associative elastic-plastic problems is missing or at least in-

complete. Especially, standard implicit discretizations of time (pseudo-time) variable lead to problematic numerical behavior. The drawbacks of the non-associative models can be suppressed by variational approaches based on theory of bipotentials [Hjiaj et al. (2003), Hamlaoui et al. (2017)] or semi-implicit time schemes [Krabbenhoft (2012)]. Within the LA method, Davis [Davis (1968)] suggested to modify the strength parameters and consequently approximate the nonassociative model by the associative one. In [Tschuchnigg et al. (2015a), Tschuchnigg et al. (2015b), Tschuchnigg et al. (2015c)], the Davis approach has been modified for purposes of the SSR method.

Inspired by the recent papers from Tschuchnigg et al. mentioned above, we suggest an optimization definition of the SSR problem that is independent of the plastic flow rule and a space discretization. Basic properties of the optimization problem are shown and duality between the static and kinematic settings of this problem is derived. Within the nonassociative plasticity, two different optimization approaches are suggested.

For numerical solution, we propose a regularization of the optimization problems inspired by recent papers [Sysala et al. (2015), Cermak et al. (2015), Haslinger et al. (2016a)], [Haslinger et al. (2016b), Repin et al. (2018), Haslinger et al. (2019), Reddy and Sysala (2020)]. Convergence with respect to the regularization parameter is analyzed in order to relate the original and regularized problems. The regularization enables to solve the problem by the standard finite element methods and by the damped Newton method suggested in [Sysala (2012)]. Mesh adaptivity is also used to achieve more accurate results. The problem is implemented within in-house Matlab codes. These codes based on elastic-plastic solvers have been systematically developed and described in [Sysala et al. (2016), Sysala et al. (2017), Cermak et al. (2019)]. Some of the codes are available for download [Cermak et al. (2018)]. For comparison of the results with standard approaches, the commercial softwares Plaxis and Comsol Multiphysics are used.

The rest of the paper is organized as follows. In Section 2, we introduce a scheme of the elastic-perfectly plastic problem with the Mohr-Coulomb yield criterion and present main ideas of the SSR and LA methods. In Section 3, the optimization definitions of these methods are introduced and compared for the associative plasticity. Section 4 is devoted to the non-associative case where the Davis approach is used and modified for purposes of the SSR method. In Section 5, variational principles, duality and the kinematic approaches to the SSR method are presented. The regularization method is introduced and analyzed in Section 6. Numerical examples illustrating the efficiency of the suggested numerical methods are presented in Section 7. Concluding remarks to the paper are introduced in Section 8. Appendix contains a closed form of the regularized dissipative function to the

Mohr-Coulomb yield criterion.

## 2 Preliminaries: the elastic-perfectly plastic Mohr-Coulomb problem and safety factors

We consider an elastic-perfectly plastic problem based on the Mohr-Coulomb yield criterion, a non-associative plastic flow rule and on monotone, proportional loading. We briefly introduce this problem and refer to [de Souza Neto et al. (2011), Sysala et al. (2017)] for more details.

It is assumed that an investigated body occupies a bounded domain  $\Omega \subset \mathbb{R}^3$  with boundary  $\partial\Omega$ . This boundary is split into two disjoint parts,  $\partial\Omega_u$  and  $\partial\Omega_f$ , where the body is fixed and the surface force  $\mathbf{f}$  is prescribed, respectively. Volume forces acting in  $\Omega$  are denoted by  $\mathbf{F}$ . Let  $\mathbf{x} \in \Omega$  and  $t \in (0, t_{\max})$  denote the space and time (pseudo-time) variables, respectively. The assumption on the monotone and proportional loading means that the volume and surface forces are in the forms

$$\mathbf{F} = t\bar{\mathbf{F}} \text{ in } \Omega, \quad \mathbf{f} = t\bar{\mathbf{f}} \text{ on } \partial\Omega_f, \quad t \in (0, t_{\max}), \quad (2.1)$$

where  $\bar{\mathbf{F}}: \Omega \rightarrow \mathbb{R}^3$  and  $\bar{\mathbf{f}}: \partial\Omega_f \rightarrow \mathbb{R}^3$  denote given forces independent of  $t$ . So the pseudo-time variable  $t$  is also the load factor.

Deformation of the body is described by the displacement vector field  $\mathbf{u}$  satisfying the boundary and initial conditions

$$\mathbf{u} = \mathbf{0} \text{ on } \partial\Omega_u \times (0, t_{\max}), \quad \mathbf{u} = \mathbf{0} \text{ in } \Omega \times \{0\}, \quad (2.2)$$

and by the infinitesimal strain  $\boldsymbol{\varepsilon}$  where

$$\boldsymbol{\varepsilon} := \boldsymbol{\varepsilon}(\mathbf{u}) = \frac{1}{2}(\nabla\mathbf{u} + (\nabla\mathbf{u})^\top). \quad (2.3)$$

The strain  $\boldsymbol{\varepsilon}$  is decomposed into elastic and plastic components  $\boldsymbol{\varepsilon}^e$  and  $\boldsymbol{\varepsilon}^p$ , respectively, according to

$$\boldsymbol{\varepsilon} = \boldsymbol{\varepsilon}^e + \boldsymbol{\varepsilon}^p. \quad (2.4)$$

The stress state of the body is represented by the symmetric Cauchy stress tensor  $\boldsymbol{\sigma}$

satisfying the equilibrium equation

$$-\operatorname{div} \boldsymbol{\sigma} = \mathbf{F}, \quad (2.5)$$

and the Neumann boundary conditions

$$\boldsymbol{\sigma} \mathbf{n} = \mathbf{f} \text{ on } \partial\Omega_f \times (0, T), \quad (2.6)$$

where  $\mathbf{n}$  denotes the outward unit normal to the boundary  $\partial\Omega$ . The stress  $\boldsymbol{\sigma}$  also satisfies the Mohr-Coulomb yield criterion

$$(\sigma_1 - \sigma_3) + (\sigma_1 + \sigma_3) \sin \phi - 2c \cos \phi \leq 0, \quad (2.7)$$

where  $\sigma_1$  and  $\sigma_3$  denote the maximal and minimal principle stresses of  $\boldsymbol{\sigma}$ , respectively,  $c$  is the cohesion and  $\phi$  denotes the friction angle. (Notice that the standard mechanical sign convection has been used.) Using the well-known formulas

$$\cos \phi = \frac{1}{\sqrt{1 + \tan^2 \phi}}, \quad \sin \phi = \frac{\tan \phi}{\sqrt{1 + \tan^2 \phi}}, \quad (2.8)$$

we arrive at the following equivalent form of the yield criterion:

$$\Phi(\boldsymbol{\sigma}) := (\sigma_1 - \sigma_3) \sqrt{1 + \tan^2 \phi} + (\sigma_1 + \sigma_3) \tan \phi - 2c \leq 0, \quad (2.9)$$

which is more appropriate for consequent analysis of the shear strength reduction (SSR) method.

The elastic-perfectly plastic model is completed by the initial-value constitutive model:

$$\left. \begin{aligned} \boldsymbol{\sigma} &= \mathbb{C}(\boldsymbol{\varepsilon} - \boldsymbol{\varepsilon}^p) && \text{in } \Omega \times (0, t_{\max}), \\ \dot{\boldsymbol{\varepsilon}}^p &\in \dot{\gamma} \partial \Psi(\boldsymbol{\sigma}) && \text{in } \Omega \times (0, t_{\max}), \\ \dot{\gamma} &\geq 0, \quad \Phi(\boldsymbol{\sigma}) \leq 0, \quad \dot{\gamma} \Phi(\boldsymbol{\sigma}) = 0, && \text{in } \Omega \times (0, t_{\max}) \\ \boldsymbol{\varepsilon}^p &= \mathbf{0} && \text{in } \Omega \times \{0\}. \end{aligned} \right\} \quad (2.10)$$

Here,

$$\Psi(\boldsymbol{\sigma}) := (\sigma_1 - \sigma_3) \sqrt{1 + \tan^2 \psi} + (\sigma_1 + \sigma_3) \tan \psi - 2c, \quad (2.11)$$

is the plastic potential,  $\psi$  if the dilatation angle,  $\gamma$  denotes the plastic multiplier, the dot symbol means the pseudo-time derivative of a quantity and  $\partial \Psi(\boldsymbol{\sigma})$  is the subdifferential

of  $\Psi$  at  $\boldsymbol{\sigma}$ . The fourth order tensor  $\mathbb{C}$  represents the linear isotropic elastic law:

$$\boldsymbol{\sigma} = \mathbb{C}\boldsymbol{\varepsilon}^e = \frac{1}{3}(3K - 2G)(\mathbf{I} : \boldsymbol{\varepsilon}^e)\mathbf{I} + 2G\boldsymbol{\varepsilon}^e, \quad (2.12)$$

where  $\mathbf{I}$  is the unit 2nd-order tensor, “ $:$ ” denotes the biscalar product and  $K, G > 0$ ,  $3K > 2G$ , denote the bulk and shear moduli, respectively.

The elastic-perfectly plastic problem is thus defined by the formulas (2.1)–(2.12). The given material parameters  $\phi$  and  $\psi$  satisfy  $0 \leq \psi \leq \phi \leq \pi/2$ . In the case  $\psi = \phi$ , we arrive at the associative model which is supported by mathematical theory based on the principle of maximum plastic dissipation, see, for example, [Han and Reddy (2012)]. Numerical methods for the associative plasticity are also more stable and simpler. For example, it is not necessary to use the arc-length control of the loading unlike the nonassociative case.

Now we sketch the main idea of the shear strength reduction (SSR) method and the limit analysis (LA) method. More precise definitions are introduced and derived in the next sections. The SSR method is based on the choice  $t_{\max} = 1$  and on a strength reduction parameter  $\lambda > 0$ . This parameter is applied on the strength parameters  $c$ ,  $\phi$  and  $\psi$  as follows:

$$c_\lambda := \frac{c}{\lambda}, \quad \phi_\lambda := \arctan \frac{\tan \phi}{\lambda}, \quad (2.13)$$

and

$$\psi_\lambda := \psi \text{ until } \psi < \phi_\lambda, \text{ then } \psi_\lambda := \phi_\lambda. \quad (2.14)$$

The corresponding factor of safety (FoS) is formally defined as a maximum of  $\lambda$  for which the elastic-perfectly plastic problem has a solution with respect to the parameters  $c_\lambda$ ,  $\phi_\lambda$ ,  $\psi_\lambda$  and  $t_{\max} = 1$ .

The FoS for the LA method can be formally defined as the maximum of the load factor  $t$  (see (2.1)) for which the elastic-perfectly plastic problem has a solution with respect to the parameters  $c$ ,  $\phi$  and  $\psi$ . This method is mostly defined for the associative problem with  $\phi = \psi$ . For the non-associative case, the strength parameters can be modified by Davis' approach in order to stabilize the computation, see Section 4.

FoS determined by the SSR and LA methods are different, in general. The SSR-FoS is usually closer to one than the LA-FoS. Therefore, if LA-FoS is close to one, one can expect that both the safety factors are almost the same. In [Tschuchnigg et al. (2015a), Tschuchnigg et al. (2015b), Tschuchnigg et al. (2015c)], a parametrization of the LA method has been proposed to be the factors LA-FoS and SSR-FoS almost the same. The parametrization will be described below in more details.

### 3 Shear strength reduction for associative plasticity and its comparison with limit analysis

In this section, we introduce the static principle of the SSR method for the associative model with  $\phi = \psi$ . In this case, it is well-known that the influence of the plastic flow rule and the elasticity tensor  $\mathbb{C}$  (see (2.10), (2.12)) is negligible on the factor of safety (FoS) for the SSR method and also for the LA method. In the following three subsections, we introduce definitions of FoS for the SSR and LA methods, analyze and compare them.

#### 3.1 Static principle of the SSR method

Let  $\lambda^*$  denote FoS for the SSR method. If we neglect the influence of the plastic flow rule and the elasticity tensor on  $\lambda^*$  then we arrive at the following time-independent definition:

$\lambda^* = \text{supremum of } \lambda \geq 0 \text{ subject to}$

$$\left. \begin{aligned} -\text{div } \boldsymbol{\sigma} &= \mathbf{F} \text{ in } \Omega, \quad \boldsymbol{\sigma} \mathbf{n} = \mathbf{f} \text{ on } \partial\Omega_f, \\ (\sigma_1 - \sigma_3) \sqrt{1 + \frac{\tan^2 \phi}{\lambda^2}} + (\sigma_1 + \sigma_3) \frac{\tan \phi}{\lambda} &\leq 2 \frac{c}{\lambda} \text{ in } \Omega. \end{aligned} \right\} \quad (3.1)$$

It means that we look for the maximum over  $\lambda$  for which there exists the stress  $\boldsymbol{\sigma}$  satisfying (3.1). In particular, the first line in (3.1) is derived from (2.5), (2.6) and is satisfied for *statically* admissible stresses. The second line is derived from (2.9), (2.13) and says that  $\boldsymbol{\sigma}$  is *plastically* admissible with respect to  $\lambda$ . According to the literature on convex analysis [Ekeland and Temam (1974), Temam (1985), Christiansen (1990)], we rather use the supremum than the maximum in this definition because for the critical value  $\lambda^*$ , the admissible stress  $\boldsymbol{\sigma}$  satisfying (3.1) need not exist on functional spaces. Although the definition admits the case  $\lambda^* = +\infty$ , one can expect that  $\lambda^*$  is finite in geotechnical practice.

Multiplying the inequality in the second line of (3.1) by  $\lambda$ , one can arrange the constraints (3.1) into the following form:

$\lambda^* = \text{supremum of } \lambda \geq 0 \text{ subject to}$

$$\left. \begin{aligned} -\text{div } \boldsymbol{\sigma} &= \mathbf{F} \text{ in } \Omega, \quad \boldsymbol{\sigma} \mathbf{n} = \mathbf{f} \text{ on } \partial\Omega_f, \\ \Phi(\lambda; \boldsymbol{\sigma}) &\leq 0 \text{ in } \Omega. \end{aligned} \right\} \quad (3.2)$$

where

$$\Phi(\lambda; \boldsymbol{\sigma}) := (\sigma_1 - \sigma_3) \sqrt{\lambda^2 + \tan^2 \phi} + (\sigma_1 + \sigma_3) \tan \phi - 2c. \quad (3.3)$$

The form (3.2) is more convenient for analysis of the SSR problem than (3.1) as we shall see below. By comparing (2.9) with (3.3) we have  $\Phi(1; \boldsymbol{\sigma}) = \Phi(\boldsymbol{\sigma})$ . The following statement is important to be the safety factor  $\lambda^*$  well defined.

**Lemma 3.1.** *If (3.2) is satisfied for some  $\lambda := \bar{\lambda} > 0$  then (3.2) holds for any  $\lambda < \bar{\lambda}$ .*

*Proof.* For any  $\boldsymbol{\sigma}$  fixed,  $\sigma_1 - \sigma_3 \geq 0$  and thus the function  $\lambda \mapsto \Phi(\lambda; \boldsymbol{\sigma})$  is nondecreasing. Hence, if there exists  $\boldsymbol{\sigma}$  such that (3.2) holds for some  $\lambda := \bar{\lambda} > 0$  then  $\boldsymbol{\sigma}$  also satisfies (3.2) for any  $\lambda < \bar{\lambda}$ .  $\square$

One can also expect in slope stability or similar problems that there exists  $\boldsymbol{\sigma}$  satisfying (3.2) for  $\lambda = 0$ , that is,

$$\begin{cases} -\operatorname{div} \boldsymbol{\sigma} = \mathbf{F} \text{ in } \Omega, \quad \boldsymbol{\sigma} \mathbf{n} = \mathbf{f} \text{ on } \partial\Omega_f, \\ \sigma_1 \tan \phi \leq c \text{ in } \Omega. \end{cases} \quad (3.4)$$

It suffices to choose the stress field derived from the solution of elastic or elastic-plastic problem. The corresponding maximal principle stress  $\sigma_1$  should be even nonpositive in  $\Omega$ .

Let us recall that the Mohr-Coulomb yield surface is the pyramid aligned with the hydrostatic axis, see, for example, [de Souza Neto et al. (2011)]. From the inequality  $\Phi(\lambda; \boldsymbol{\sigma}) \leq 0$  and (3.3), it is possible to see that its apex is independent of  $\lambda$ . By reducing the strength parameters (i.e., by enlarging  $\lambda$ ) the slope of the Mohr-Coulomb pyramid is reduced. For  $\lambda \rightarrow 0$ , the pyramid varies to a half-space.

## 3.2 The LA method and its comparison with the SSR method

Although this paper is focused on the SSR method, we also introduce the LA method and compare them in order to generalize the Davis approach for the SSR method, see the next section.

Let  $\zeta^*$  denote FoS for the LA method. This value is defined as follows:

$\zeta^* = \text{supremum of } \zeta \geq 0 \text{ subject to}$

$$\left. \begin{aligned} -\text{div } \boldsymbol{\sigma} &= \zeta \mathbf{F} \text{ in } \Omega, \quad \boldsymbol{\sigma} \mathbf{n} = \zeta \mathbf{f} \text{ on } \partial\Omega_f, \\ (\sigma_1 - \sigma_3) \sqrt{1 + \tan^2 \phi} + (\sigma_1 + \sigma_3) \tan \phi &\leq 2c \text{ in } \Omega. \end{aligned} \right\} \quad (3.5)$$

Let us note that the parameter  $\zeta$  is applied on the external forces and  $\zeta^*$  is also called the limit load factor. The definition above is the static principle of LA which is also known in literature as the *lower bound theorem of LA* because for any  $\zeta < \zeta^*$  there exists  $\boldsymbol{\sigma}$  satisfying (3.5). Further, the second line in (3.5) can be written in the form

$$\Phi(\boldsymbol{\sigma}) = \Phi(1; \boldsymbol{\sigma}) \leq 0 \text{ in } \Omega, \quad (3.6)$$

see (2.9) and (3.3). The LA problem is well-defined from the following reasons:

1.  $\boldsymbol{\sigma} = \mathbf{0}$  satisfies the constraints (3.5) for  $\zeta = 0$ .
2. If (3.5) is satisfied for some  $\zeta := \bar{\zeta} > 0$  then (3.5) holds for any  $\zeta < \bar{\zeta}$ . Indeed, if  $\boldsymbol{\sigma}$  satisfies (3.5) for some  $\zeta := \bar{\zeta} > 0$  then  $(\zeta/\bar{\zeta})\boldsymbol{\sigma}$  satisfies (3.5) for any  $\zeta < \bar{\zeta}$ .

The value  $\zeta^* = +\infty$  is expected for larger values of the friction angle, in particular for  $\phi \geq 45^\circ$ . It is also well-known that  $\zeta^*$  depends linearly on the cohesion. Indeed, by the substitution  $\boldsymbol{\sigma} := \zeta \boldsymbol{\sigma}$ , one can rewrite the LA problem as follows:

$\zeta^* = \text{supremum of } \zeta \geq 0 \text{ subject to}$

$$\left. \begin{aligned} -\text{div } \boldsymbol{\sigma} &= \mathbf{F} \text{ in } \Omega, \quad \boldsymbol{\sigma} \mathbf{n} = \mathbf{f} \text{ on } \partial\Omega_f, \\ (\sigma_1 - \sigma_3) \sqrt{1 + \tan^2 \phi} + (\sigma_1 + \sigma_3) \tan \phi &\leq 2\frac{c}{\zeta} \text{ in } \Omega. \end{aligned} \right\} \quad (3.7)$$

Hence, if  $\zeta^*$  is the limit load factor for the cohesion  $c$  then  $\alpha\zeta^*$  is the limit value corresponding to  $\alpha c$  for any  $\alpha > 0$ . From (3.7), we also see that the proportional enlarging of the external forces  $\mathbf{f}$  and  $\mathbf{F}$  is equivalent to the reduction of the cohesion. During this reduction, the apex of the Mohr-Coulomb pyramid is moved to the origin of the coordinates but the shape of the pyramid remains the same unlike the SSR method.

### 3.3 Comparison of the SRR and LA methods

In order to compare the SRR and LA methods, we arise from (3.7) and parametrize the LA problem as follows:

given  $\lambda > 0$ , find  $\ell(\lambda) = \sup_{\zeta \geq 0} \zeta$  subject to

$$\left. \begin{array}{l} -\operatorname{div} \boldsymbol{\sigma} = \mathbf{F} \text{ in } \Omega, \quad \boldsymbol{\sigma} \mathbf{n} = \mathbf{f} \text{ on } \partial\Omega_f, \\ (\sigma_1 - \sigma_3) \sqrt{\lambda^2 + \tan^2 \phi} + (\sigma_1 + \sigma_3) \tan \phi \leq 2\frac{c}{\zeta} \text{ in } \Omega. \end{array} \right\} \quad (3.8)$$

We shall analyze properties of the function  $\ell$ . Clearly,  $\zeta^* = \ell(1)$ .

**Lemma 3.2.** *The function  $\ell$  is nonincreasing.*

*Proof.* Let  $\lambda_1 \leq \lambda_2$  and  $\zeta \geq 0$  be an arbitrary value satisfying  $\zeta < \ell(\lambda_2)$ . Then there exists  $\boldsymbol{\sigma}$  satisfying (3.8) for  $\lambda := \lambda_2$ . Since the function  $\lambda \mapsto \sqrt{\lambda^2 + \tan^2 \phi}$  is increasing, it is easy to see that  $\boldsymbol{\sigma}$  satisfies (3.8) also for  $\lambda := \lambda_1$ . Therefore,  $\zeta \leq \ell(\lambda_1)$  and consequently  $\ell(\lambda_1) \geq \ell(\lambda_2)$ .  $\square$

For reasonable settings of the problem, one can also expect that  $\ell$  is continuous and decreasing. By analysis of the constraints (3.8), we deduce that  $\ell(0) = +\infty$  and  $\ell(\lambda) \rightarrow 0$  as  $\lambda \rightarrow +\infty$ . The mentioned properties of the function  $\ell$  are sketched in Figure 1.

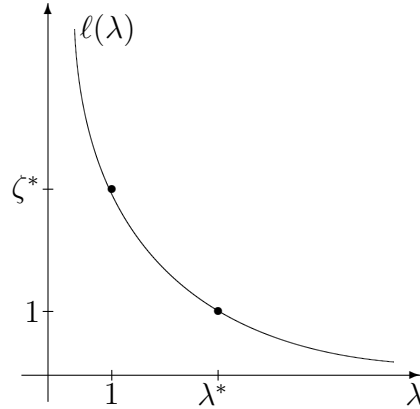


Figure 1: Scheme of the function  $\ell$  enabling to compare the safety factors for the SSR and LA methods.

By comparison of the constraints (3.2) and (3.8), we derive that the SSR-based safety parameter  $\lambda^*$  defined in Section 3.1 is a unique solution of the following equation:

$$\ell(\lambda^*) = 1. \quad (3.9)$$

It means that the safety factor  $\lambda^*$  can be found by the parametrization of the limit analysis problem. From (3.9) and the properties of  $\ell$ , we have:

- $\lambda^* = 1$  if and only if  $\zeta^* = 1$ ;
- if  $\lambda^* > 1$  if and only if  $\zeta^* > 1$ ;
- if  $\lambda^* < 1$  if and only if  $\zeta^* < 1$ .

In practice, it is observed that  $\lambda^*$  is closer to one than  $\zeta^*$ . One can expect that the difference between  $\lambda^*$  and  $\zeta^*$  is significant for  $\phi \approx 45^\circ$  when  $\zeta^*$  is too large, see Section 3.2.

Finally of this section, we show that it suffices to parametrize only the friction angle within the LA method in order to compute the SSR factor  $\lambda^*$ . Indeed, consider a parameter  $\chi \geq 0$  and define the following problem:

$\tilde{\ell}(\chi) = \text{supremum of } \zeta \geq 0 \text{ subject to}$

$$\left. \begin{array}{l} -\operatorname{div} \boldsymbol{\sigma} = \mathbf{F} \text{ in } \Omega, \quad \boldsymbol{\sigma} \mathbf{n} = \mathbf{f} \text{ on } \partial\Omega_f, \\ (\sigma_1 - \sigma_3) \sqrt{1 + \frac{\tan^2 \phi}{\chi^2}} + (\sigma_1 + \sigma_3) \frac{\tan \phi}{\chi} \leq 2 \frac{c}{\zeta} \text{ in } \Omega. \end{array} \right\} \quad (3.10)$$

Since the LA-based safety factor depends linearly on the cohesion, it is easy to prove that

$$\ell(\lambda) = \frac{1}{\lambda} \tilde{\ell}(\lambda) \quad \forall \lambda \geq 0. \quad (3.11)$$

From (3.9) and (3.11), it follows that the SSR factor of safety  $\lambda^*$  can be found as a solution of the fixed-point problem

$$\tilde{\ell}(\lambda^*) = \lambda^*. \quad (3.12)$$

One can suppose that the function  $\tilde{\ell}$  is also decreasing in slope stability or similar geo-application. Under this assumption it is possible to prove  $\lambda^*$  is closer to one than  $\zeta^*$ .

Using the equations  $\ell(\lambda^*) = 1$  or  $\tilde{\ell}(\lambda^*) = \lambda^*$  and a solver on the LA problem, one can compute the safety factor  $\lambda^*$  of the SSR method. In fact, such a treatment was used in [Tschuchnigg et al. (2015a), Tschuchnigg et al. (2015b), Tschuchnigg et al. (2015c)]. In Section 6, we shall propose another numerical method for finding  $\lambda^*$  without the necessity to solve repeatedly the LA problem.

## 4 Modified Davis approach for the shear strength reduction method in non-associative plasticity

In order to use the limit analysis (LA) method for the non-associative model with  $\psi < \phi$ , it was suggested [Davis (1968)] to reduce the strength parameters by the following empirical formulas:

$$c_\beta := \beta c, \quad \phi_\beta = \psi_\beta := \arctan(\beta \tan \phi), \quad (4.1)$$

where

$$\beta := \frac{\cos \psi \cos \phi}{1 - \sin \psi \sin \phi}, \quad (4.2)$$

and then solve the LA problem with  $c_\beta$  and  $\phi_\beta = \psi_\beta$ . Notice that  $\beta = 1$  for  $\psi = \phi$ . In order to apply a similar approach for the shear strength reduction (SSR) method, we use the function  $\ell$  introduced in Section 3.3 which parametrizes the LA problem with respect to the strength reduction factor  $\lambda$ . However, this parametrization causes that the factor  $\beta$  depends on  $\lambda$  and thus the modification of the Davis approach for purposes of the SSR method is not so straightforward.

In [Tschuchnigg et al. (2015b)], three different modifications of the Davis approach have been proposed. The aim of this section is to analyze in more details two of these modifications. To this end, we use the static principle presented in Section 3.1.

### 4.1 Davis approach I for the non-associative SSR method

In the first approach (called Davis A in [Tschuchnigg et al. (2015b)]), we assume that the parameter  $\beta$  defined by (4.2) remains fixed. We denote the corresponding FoS of the SSR method by  $\lambda_I^*$  and define it as follows:

$\lambda_I^* = \text{supremum of } \lambda \geq 0 \text{ subject to}$

$$\left. \begin{aligned} -\operatorname{div} \boldsymbol{\sigma} &= \mathbf{F} \quad \text{in } \Omega, \quad \boldsymbol{\sigma} \mathbf{n} = \mathbf{f} \quad \text{on } \partial\Omega_f, \\ (\sigma_1 - \sigma_3) \sqrt{1 + \frac{\beta^2 \tan^2 \phi}{\lambda^2}} + (\sigma_1 + \sigma_3) \frac{\beta \tan \phi}{\lambda} &\leq 2 \frac{\beta c}{\lambda} \quad \text{in } \Omega. \end{aligned} \right\} \quad (4.3)$$

Using the function  $\Phi$  (see (3.3)), one can also write

$\lambda_I^* = \text{supremum of } \lambda \geq 0 \text{ subject to}$

$$\left. \begin{array}{l} -\operatorname{div} \boldsymbol{\sigma} = \mathbf{F} \text{ in } \Omega, \quad \boldsymbol{\sigma} \mathbf{n} = \mathbf{f} \text{ on } \partial\Omega_f, \\ \Phi\left(\frac{\lambda}{\beta}; \boldsymbol{\sigma}\right) \leq 0 \text{ in } \Omega. \end{array} \right\} \quad (4.4)$$

If we compare the definitions of  $\lambda^*$  (see Section 3.1) and  $\lambda_I^*$ , use the properties of  $\Psi$  and the fact that  $\beta \leq 1$ , then we arrive at the expected inequality

$$\lambda_I^* \leq \lambda^* \quad (4.5)$$

saying that FoS decreases with the decreasing dilatation angle  $\psi$ . Using the function  $\ell$  defined in Section 3.3, one can find  $\lambda_I^*$  as a solution of the following implicit equation:

$$\ell\left(\frac{\lambda_I^*}{\beta}\right) = 1. \quad (4.6)$$

## 4.2 Davis approach II for the non-associative SSR method

In the second approach (called Davis C in [Tschuchnigg et al. (2015b)]), we assume that the parameter  $\beta$  depends on the strength reduction factor  $\lambda \geq 0$ . This dependence can be represented by the following function:

$$b(\lambda) = \begin{cases} \frac{\cos \psi \cos \phi_\lambda}{1 - \sin \psi \sin \phi_\lambda}, & \text{if } \phi_\lambda \geq \psi, \\ 1, & \text{if } \phi_\lambda \leq \psi, \end{cases} \quad (4.7)$$

where the function  $\lambda \mapsto \phi_\lambda$  is defined by (2.13). Clearly,  $\beta = b(1)$ . Further, it is easy to show that the function  $b$  is continuous, nondecreasing and bounded by one from above.

We denote the FoS of the SSR method for approach II by  $\lambda_{II}^*$  and define it as follows:

$\lambda_{II}^* = \text{supremum of } \lambda \geq 0 \text{ subject to}$

$$\left. \begin{array}{l} -\operatorname{div} \boldsymbol{\sigma} = \mathbf{F} \text{ in } \Omega, \quad \boldsymbol{\sigma} \mathbf{n} = \mathbf{f} \text{ on } \partial\Omega_f, \\ \Phi\left(\frac{\lambda}{b(\lambda)}; \boldsymbol{\sigma}\right) \leq 0 \text{ in } \Omega. \end{array} \right\} \quad (4.8)$$

The following statement is important to be the safety factor  $\lambda_{II}^*$  well defined.

**Lemma 4.1.** *If (4.8) is satisfied for some  $\lambda := \bar{\lambda} > 0$  then (4.8) holds for any  $\lambda < \bar{\lambda}$ .*

*Proof.* Using the formulas (2.8), we derive that

$$\frac{\lambda}{b(\lambda)} = \begin{cases} \frac{\sqrt{\lambda^2 + \tan^2 \phi} - \tan \phi \sin \psi}{\cos \psi}, & \text{if } \phi_\lambda \geq \psi, \\ \lambda, & \text{if } \phi_\lambda \leq \psi, \end{cases} \quad (4.9)$$

implying that the function  $\lambda \mapsto \lambda/b(\lambda)$  is continuous, increasing and nonnegative.

Let  $\bar{\lambda} > 0$  be such that there exists  $\sigma$  satisfying (4.8) for  $\lambda := \bar{\lambda} > 0$ . For any  $\lambda < \bar{\lambda}$ , we have

$$\Phi\left(\frac{\lambda}{b(\lambda)}; \sigma\right) \leq \Phi\left(\frac{\bar{\lambda}}{b(\bar{\lambda})}; \sigma\right) \leq 0 \quad \text{in } \Omega.$$

Therefore,  $\sigma$  satisfies (4.8) for any  $\lambda < \bar{\lambda}$ .  $\square$

If we compare the definitions of  $\lambda^*$  (see Section 3.1) and  $\lambda_{II}^*$ , use the properties of  $\Psi$  and the fact that  $b(\lambda) \leq 1$  for any  $\lambda \geq 0$ , then we arrive at the expected inequality

$$\lambda_{II}^* \leq \lambda^*. \quad (4.10)$$

Using the function  $\ell$  defined in Section 3.3, one can find  $\lambda_{II}^*$  as a solution of the following implicit equation:

$$\ell\left(\frac{\lambda_{II}^*}{b(\lambda_{II}^*)}\right) = 1. \quad (4.11)$$

One can also relate the safety factors  $\lambda_I^*$  and  $\lambda_{II}^*$ . We have:

- $\lambda_I^* = 1$  if and only if  $\lambda_{II}^* = 1$ ;
- if  $\lambda_I^* > 1$  then  $\lambda_I^* \leq \lambda_{II}^*$ ;
- if  $\lambda_I^* < 1$  then  $\lambda_I^* \geq \lambda_{II}^*$ .

## 5 Variational principles, duality and kinematic approaches

The numerical methods presented below are rather based on the kinematic principle to the SSR method. Therefore, we derive this dual formulation of the SSR problem. The derivation is similar to the one in the limit analysis problem [Temam (1985), Christiansen (1990),

Haslinger et al. (2019)]. Therefore, some steps of the derivation will be skipped, for the sake of simplicity.

First, we unify the notation of the problems defining the safety factors  $\lambda^*$ ,  $\lambda_I^*$  and  $\lambda_{II}^*$  in the following way:

$\omega^* = \text{supremum of } \lambda \geq 0 \text{ subject to}$

$$\left. \begin{array}{l} -\operatorname{div} \boldsymbol{\sigma} = \mathbf{F} \text{ in } \Omega, \quad \boldsymbol{\sigma} \mathbf{n} = \mathbf{f} \text{ on } \partial\Omega_f, \\ \Phi(q(\lambda); \boldsymbol{\sigma}) \leq 0 \text{ in } \Omega, \end{array} \right\} \quad (5.1)$$

where  $q$  is an increasing, continuous and nonnegative function. Setting  $q(\lambda) = \lambda$ ,  $q(\lambda) = \lambda/\beta$  and  $q(\lambda) = \lambda/b(\lambda)$ , we obtain  $\omega^* = \lambda^*$ ,  $\omega^* = \lambda_I^*$  and  $\omega^* = \lambda_{II}^*$ , respectively.

Next, we introduce the following functional spaces:

$$V = \{\mathbf{v} \in [H^1(\Omega)]^3 \mid \mathbf{v} = 0 \text{ on } \partial\Omega_u\}, \quad (5.2)$$

$$\Sigma = \{\boldsymbol{\sigma} \in [L^2(\Omega)]^{3 \times 3} \mid \sigma_{ij} = \sigma_{ji} \text{ in } \Omega\}. \quad (5.3)$$

The space  $V$  represents velocity fields satisfying the Dirichlet boundary condition from (2.2) and  $\Sigma$  is used for symmetric stress fields.  $L^2(\Omega)$  and  $H^1(\Omega)$  denotes the Lebesgue and Sobolev spaces, respectively, with respect to square integrable functions. More advanced functional spaces are considered in [Christiansen (1990)].

Using the space  $V$  we arrive at the weak form of (5.1)<sub>1</sub>:

$$\int_{\Omega} \boldsymbol{\sigma} : \boldsymbol{\varepsilon}(\mathbf{v}) \, dx = L(\mathbf{v}) \quad \forall \mathbf{v} \in V, \quad (5.4)$$

where  $L$  is the load functional defined by

$$L(\mathbf{v}) = \int_{\Omega} \mathbf{F} \cdot \mathbf{v} \, dx + \int_{\partial\Omega_f} \mathbf{f} \cdot \mathbf{v} \, ds. \quad (5.5)$$

To be the integrals in (5.5) meaningful, it suffices to assume that the components of  $\mathbf{F}$  and  $\mathbf{f}$  belong to the  $L^2$  space. Let  $\Lambda$  denote the set of stresses  $\boldsymbol{\sigma} \in \Sigma$  satisfying (5.4) and let

$$P_{q(\lambda)} := \{\boldsymbol{\sigma} \in \Sigma \mid \Phi(q(\lambda); \boldsymbol{\sigma}) \leq 0 \text{ in } \Omega\}. \quad (5.6)$$

We see that the set  $P_{q(\lambda)}$  represents the constraint (5.1)<sub>2</sub> and thus we can write

$$\begin{aligned}\omega^* &= \sup\{\lambda \geq 0 \mid P_{q(\lambda)} \cap \Lambda \neq \emptyset\} \\ &= \sup_{\lambda \geq 0} \sup_{\sigma \in P_{q(\lambda)} \cap \Lambda} \{\lambda\}.\end{aligned}\quad (5.7)$$

From (5.4), we have

$$\inf_{v \in V} \left[ \int_{\Omega} \sigma : \varepsilon(v) dx - L(v) \right] = \begin{cases} 0, & \text{if } \sigma \in \Lambda, \\ -\infty, & \text{otherwise.} \end{cases}$$

Hence, one can rewrite (5.7) as follows:

$$\begin{aligned}\omega^* &= \sup_{\lambda \geq 0} \sup_{\sigma \in P_{q(\lambda)}} \inf_{v \in V} \left[ \lambda + \int_{\Omega} \sigma : \varepsilon(v) dx - L(v) \right] \\ &= \sup_{\lambda \geq 0} \inf_{v \in V} \sup_{\sigma \in P_{q(\lambda)}} \left[ \lambda + \int_{\Omega} \sigma : \varepsilon(v) dx - L(v) \right] \\ &= \sup_{\lambda \geq 0} \inf_{v \in V} \left[ \lambda + \int_{\Omega} D(q(\lambda); \varepsilon(v)) dx - L(v) \right],\end{aligned}\quad (5.8)$$

where

$$D(q(\lambda); \varepsilon) = \sup_{\substack{\sigma \in \mathbb{R}_{sym}^{3 \times 3} \\ \Phi(q(\lambda); \sigma) \leq 0}} \sigma : \varepsilon \quad (5.9)$$

denotes the local dissipation function depending on  $\lambda \geq 0$ . The function  $D(q(\lambda); \cdot)$  is finite-valued only on a convex cone belonging to  $\mathbb{R}_{sym}^{3 \times 3}$ . Therefore, the inner problem in (5.8) can be classified as cone programming. The problem (5.8) can be interpreted as the *kinematic principle* to the SSR method.

Let us note that the ordering of inf and sup has been interchanged during the derivation of (5.8). The corresponding equality is expected and partially supported by the results presented in [Christiansen (1990), Haslinger et al. (2019)].

## 6 Regularization method

In [Sysala et al. (2015), Cermak et al. (2015), Haslinger et al. (2016a), Haslinger et al. (2016b), Repin et al. (2018), Haslinger et al. (2019)], a regularization method has been systematically developed for solution of the limit analysis (LA) problem. This method has also

been used in strain-gradient plasticity [Reddy and Sysala (2020)]. The aim of this section is to use the regularization for solution of the shear strength reduction (SSR) problem and study the relation between the original and the regularized problem.

We arise from (5.7) and regularize this problem with respect to a parameter  $\alpha > 0$  as follows:

$$\omega_\alpha^* = \sup_{\lambda \geq 0} \sup_{\boldsymbol{\sigma} \in P_{q(\lambda)} \cap \Lambda} \left[ \lambda - \frac{1}{2\alpha} \int_{\Omega} \mathbb{C}^{-1} \boldsymbol{\sigma} : \boldsymbol{\sigma} dx \right], \quad (6.1)$$

where  $\mathbb{C}$  is a positive definite fourth order tensor, for example, the elastic tensor from (2.12). We have the following result.

**Lemma 6.1.** *The sequence  $\{\omega_\alpha^*\}_{\alpha > 0}$  defined by (6.1) is nondecreasing and satisfying*

$$\omega_\alpha^* \leq \omega^*, \quad \lim_{\alpha \rightarrow +\infty} \omega_\alpha^* = \omega^*, \quad (6.2)$$

where  $\omega^*$  is defined by (5.7).

*Proof.* It is readily seen that the inequalities  $\omega_{\alpha_1}^* \leq \omega_{\alpha_2}^* \leq \omega^*$  hold for any  $0 < \alpha_1 \leq \alpha_2$ . Next, for any  $\lambda < \omega^*$  the intersection  $P_{q(\lambda)} \cap \Lambda$  is nonempty as follows from (5.7). Then the inner sup-problem in (6.1) has a unique solution  $\boldsymbol{\sigma}_\lambda \in P_{q(\lambda)} \cap \Lambda$  because it contains the quadratic functional. Consequently,

$$\lim_{\alpha \rightarrow +\infty} \omega_\alpha^* \geq \lim_{\alpha \rightarrow +\infty} \left[ \lambda - \frac{1}{2\alpha} \int_{\Omega} \mathbb{C}^{-1} \boldsymbol{\sigma}_\lambda : \boldsymbol{\sigma}_\lambda dx \right] = \lambda$$

and thus

$$\omega^* \geq \lim_{\alpha \rightarrow +\infty} \omega_\alpha^* \geq \sup\{\lambda \geq 0 \mid P_{q(\lambda)} \cap \Lambda \neq \emptyset\} = \omega^*.$$

This implies the limit in (6.2).  $\square$

One can also write

$$\omega_\alpha^* = \max_{\lambda \geq 0} [\lambda - G_\alpha(\lambda)] = \lambda_\alpha^* - G_\alpha(\lambda_\alpha^*), \quad (6.3)$$

where

$$G_\alpha(\lambda) = \inf_{\boldsymbol{\sigma} \in P_{q(\lambda)} \cap \Lambda} \frac{1}{2\alpha} \int_{\Omega} \mathbb{C}^{-1} \boldsymbol{\sigma} : \boldsymbol{\sigma} dx \quad (6.4)$$

$$= \begin{cases} \frac{1}{2\alpha} \int_{\Omega} \mathbb{C}^{-1} \boldsymbol{\sigma}_\lambda : \boldsymbol{\sigma}_\lambda dx, & \text{if } P_{q(\lambda)} \cap \Lambda \neq \emptyset, \\ +\infty, & \text{otherwise,} \end{cases} \quad (6.5)$$

and  $\lambda_\alpha^*$  maximizes the middle term in (6.3). Since the value  $G_\alpha(\lambda_\alpha^*)$  is finite, we have  $P_{q(\lambda_\alpha^*)} \cap \Lambda \neq \emptyset$ . This fact, (5.7) and (6.3) imply the following result.

**Lemma 6.2.** *The sequence  $\{\lambda_\alpha^*\}_{\alpha>0}$  defined by (6.4) satisfies*

$$\omega_\alpha^* \leq \lambda_\alpha^* \leq \omega^*, \quad \lim_{\alpha \rightarrow +\infty} \lambda_\alpha^* = \omega^*, \quad (6.6)$$

where  $\omega^*$  and  $\omega_\alpha^*$  are defined by (5.7) and (6.1), respectively.

In practice, we observe that the value  $\lambda_\alpha^*$  is sufficiently close to  $\omega^*$  for much smaller  $\alpha$  than  $\omega_\alpha^*$ . Therefore, the sequence  $\{\lambda_\alpha^*\}_\alpha$  is more convenient for the approximation of  $\omega^*$  than  $\{\omega_\alpha^*\}_\alpha$ .

Let us note that the 1D optimization problem in (6.3) can be solved, for example, by sequential enlarging of  $\lambda$  for fixed  $\alpha$ . It is convenient to use a continuation over  $\alpha$  to be  $\lambda_\alpha^*$  sufficiently close to  $\omega^*$ . The sufficiently large value of  $\alpha$  can be found by the continuation on a coarse finite element mesh and then used on finer meshes.

Next, for solution of (6.3), it is crucial to evaluate the function  $G_\alpha$ . To this end, we use a similar duality approach as in Section 5. We arrive at the following kinematic definition of  $G_\alpha$ :

$$G_\alpha(\lambda) = - \inf_{\mathbf{v} \in V} \left[ \int_{\Omega} D_\alpha(q(\lambda); \boldsymbol{\varepsilon}(\mathbf{v})) dx - L(\mathbf{v}) \right], \quad (6.7)$$

where

$$D_\alpha(q(\lambda); \boldsymbol{\varepsilon}) = \sup_{\substack{\boldsymbol{\sigma} \in \mathbb{R}_{sym}^{3 \times 3} \\ \Phi(q(\lambda); \boldsymbol{\sigma}) \leq 0}} \left[ \boldsymbol{\sigma} : \boldsymbol{\varepsilon} - \frac{1}{2\alpha} \mathbb{C}^{-1} \boldsymbol{\sigma} : \boldsymbol{\sigma} \right] \quad (6.8)$$

is the regularized dissipative function. In particular,  $D_\alpha$  is finite-valued and differentiable with respect to  $\boldsymbol{\varepsilon}$  unlike the original dissipation  $D$ , see, for example, [Sysala (2014)]. Moreover, the second derivative of  $D_\alpha$  exists almost everywhere. Let  $T_\alpha(q(\lambda); \boldsymbol{\varepsilon}) \in \mathbb{R}_{sym}^{3 \times 3}$  denote the derivative of  $D_\alpha(q(\lambda); \boldsymbol{\varepsilon})$  with respect to  $\boldsymbol{\varepsilon}$ . Then the problem (6.7) is equivalent to the following nonlinear variational equation:

$$\text{find } \mathbf{v}_{q(\lambda)} \in V : \quad \int_{\Omega} T_\alpha(q(\lambda); \boldsymbol{\varepsilon}(\mathbf{v}_{q(\lambda)})) : \boldsymbol{\varepsilon}(\mathbf{v}) dx = L(\mathbf{v}) \quad \forall \mathbf{v} \in V. \quad (6.9)$$

It is convenient to solve it by a non-smooth and damped version of the Newton method suggested in [Sysala (2012)] because this method also finds descent directions of the functional in (6.7) which need not be bounded from below for some  $\lambda$ .

Let  $D_1 := D_\alpha$  and  $T_1 := T_\alpha$  for  $\alpha = 1$ . Then the following formulas hold for any  $\alpha > 0$ ,

$\lambda \geq 0$  and  $\boldsymbol{\varepsilon} \in \mathbb{R}_{sym}^{3 \times 3}$ :

$$D_\alpha(q(\lambda); \boldsymbol{\varepsilon}) = \frac{1}{\alpha} D_1(q(\lambda); \alpha \boldsymbol{\varepsilon}), \quad T_\alpha(q(\lambda); \boldsymbol{\varepsilon}) = T_1(q(\lambda); \alpha \boldsymbol{\varepsilon}). \quad (6.10)$$

This formulas simplifies the construction of the operators  $D_\alpha$  and  $T_\alpha$  if the continuation over  $\alpha$  is used. In addition,  $T_1$  is practically the same as the operator which arises from the implicit Euler discretization of the constitutive problem (2.10). Its construction can be found e.g. in [de Souza Neto et al. (2011), Sysala et al. (2017)]. The closed form of  $D_1$  is introduced in Appendix of this paper, for the sake of completeness.

## 7 Numerical examples

In this section, we present two different numerical examples on slope stability problems. The first example is a model homogeneous slope presented in [Tschuchnigg et al. (2015b)]. The aim is to illustrate our theoretical results and verified that the computed FoS are in accordance with the published ones. The second example arises from analysis of a real slope. A heterogeneous material and the influence of the water pore pressure are considered.

### 7.1 Softwares and their numerical solution

We use and compare the results from three different softwares: in-house codes in Matlab, Plaxis and Comsol Multiphysics.

The in-house Matlab codes are based on elastic-plastic solvers, the finite element method and on mesh adaptivity. They have been systematically developed and described in [Sysala et al. (2016), Sysala et al. (2017), Cermak et al. (2019)]. Some of the codes are available for download [Cermak et al. (2018)]. Within these codes, we have implemented the regularization method from Section 6 to achieve safety factors for the associative plasticity and for the Davis I and Davis II approaches to the nonassociative plasticity. In particular, P2 finite elements with the 7-point Gauss quadrature have been used and combined with the mesh adaptivity introduced in [Haslinger et al. (2019), Sysala et al. (2019)].

The software Plaxis enables to solve the shear strength reduction method for both associative and nonassociative plasticity. Their standard solver is based on the implicit Euler time discretization, P4 elements (in 2D) and on the arc-length method [Brinkgreve (2011)].

One can also easily implement the Davis I approach there. Due to this software we are able to compare suggested and current approaches to the shear strength reduction (SSR) method.

The software Comsol Multiphysics with its Geomechanical module is not specialized neither on the shear strength reduction method nor the arc-length method. On the other hand, one can add a global equation to the elastic-plastic system of equations with respect to an unknown parameter and optimize it. Due to these facts, the SSR method for the associative plasticity and the Davis I, II modifications can be implemented there. Beside the regularization method, the standard incremental procedure for solution of the elastic-plastic problem has been used. P4 elements are considered.

## 7.2 Homogeneous slope

Following [Tschuchnigg et al. (2015b)], we consider a homogeneous model slope depicted in Figure 2. Its inclination is  $45^\circ$  and sizes (in meters) are introduced in the figure. The (effective) friction angle  $\phi$  is  $45^\circ$ , the (effective) cohesion  $c$  is 6.0 kPa and the unit weight  $\gamma$  is 20.0 kN/m<sup>3</sup>. The dilatancy angle is either  $\psi = 0^\circ$  (nonassociative case) or  $\psi = 45^\circ$  (associative case). We have chosen such values of  $\phi$  and  $\psi$  in order to highlight maximal possible differences between the associative and nonassociative models or between the suggested and current approaches to the SSR method.

Next, we set the following values of the Young modulus and the Poisson ratio:  $E = 40$  MPa and  $\nu = 0.3$ . For purposes of the regularization method, the value  $\alpha = 1000$  is used. This value is sufficiently large as follows from Figure 5.

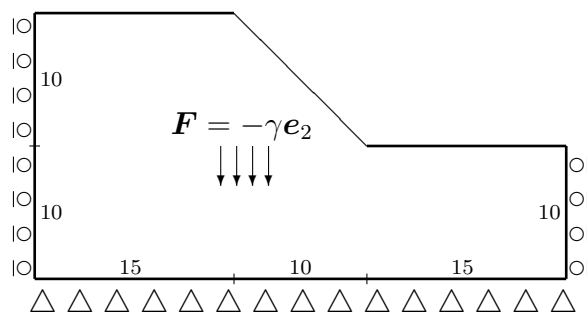


Figure 2: Geometry of the model slope with inclination 45°.

Table 1 summarizes computed factors of safety by different softwares and different approaches. These values are practically the same as in [Tschuchnigg et al. (2015b)]. The

last line contains the value of the current approach to the SSR method. The corresponding safety factor cannot be uniquely determined for finer meshes due to the oscillation of the method, see [Tschuchnigg et al. (2015b)] for more details.

Table 1: Safety factors for the homogeneous slope and different approaches

	MATLAB	COMSOL	Plaxis
$\psi = \phi$ , assoc. model	1.53	1.52	1.51
$\psi = 0^\circ$ , Davis I	1.08	1.08	1.08
$\psi = 0^\circ$ , Davis II	1.15	1.16	—
$\psi = 0^\circ$ , current approach	—	—	1.27–1.35

On the other hand, the results for the associative plasticity and for the Davis approaches are practically insensitive if sufficiently fine meshes are used. It is illustrated in Figure 3 where the mesh adaptivity within the in-house Matlab codes is used. In particular, 20 levels of meshes is considered and the corresponding safety factors remain almost constant. The finest mesh and the corresponding slip zone for the Davis II approach are depicted in Figure 4. The slip zone is visualized using the deviatoric strain.

The dependence of  $\lambda_\alpha^*$  and  $\omega_\alpha^*$  (see Section 6) for the Davis II approach on the regularization parameter  $\alpha$  is depicted in Figure 5. We see that these curves are increasing and tending to the limit value  $\omega^*$ . It confirms the theoretical results of the regularization method. We also see that  $\lambda_\alpha^*$  approximates the safety factor  $\omega^*$  even for relatively small  $\alpha$ . On the other hand, much larger values of  $\alpha$  has to be used in order to approximate  $\omega^*$  by  $\omega_\alpha^*$ .

### 7.3 Heterogeneous slope from locality Doubrava-Kozinec

The second example follows from analysis of a real slope in locality Doubrava-Kozinec (near Karvina in the North-East part of the Czech Republic) where a landslide has been observed. In Figure 6, the investigated slope profile is illustrated. We see that the slope is heterogeneous. Particular materials and their parameters are specified in Table 2. The level of groundwater is estimated by the blue curve in the figure. We distinguish the specific weights  $\gamma_{\text{unsat}}$  and  $\gamma_{\text{sat}}$  for unsaturated and saturated materials, respectively. The values of the dilatancy angle have not been available for us, therefore, we set  $\psi = 0^\circ$  for all materials. Nevertheless, we also consider the associative case with  $\psi = \phi$  in order to analyze the influence of the dilatancy.

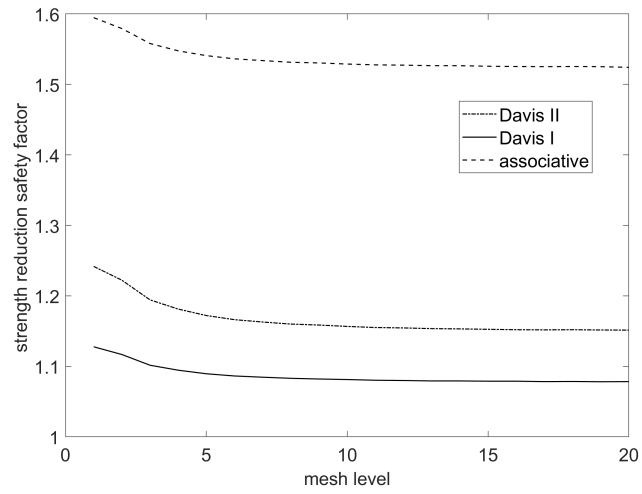


Figure 3: Safety factors for the homogeneous slope depending on mesh adaptivity.

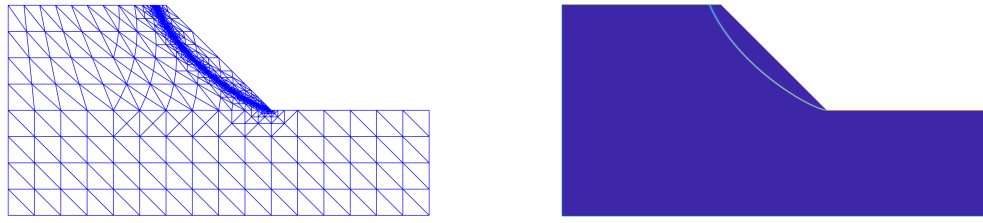


Figure 4: The finest mesh and the corresponding slip zone for the homogeneous slope.

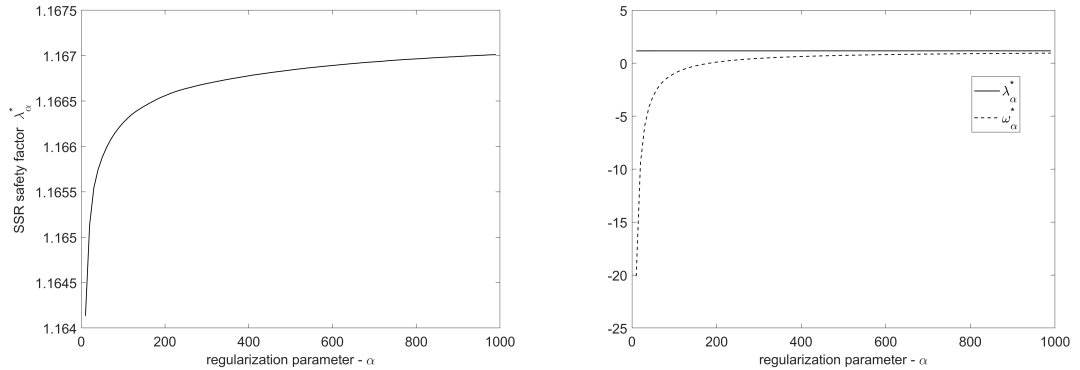


Figure 5: Dependence of  $\lambda_\alpha^*$  and  $\omega_\alpha^*$  on the regularization parameter  $\alpha$ .

Table 2: Material parameters for the heterogeneous slope.

	neogene clay	gravel	quaternary clay	sand	clayed sand
$\phi$ [°]	26	45	13	33	27
$c$ [kPa]	9	1	3	2	5
$E$ [MPa]	16	140	10	14	27
$\nu$	0.40	0.20	0.40	0.28	0.35
$\gamma_{\text{unsat}}$ [kN/m <sup>3</sup> ]	20.3	20.5	20.0	19.0	19.4
$\gamma_{\text{sat}}$ [kN/m <sup>3</sup> ]	20.7	20.6	20.5	20.5	21.4

The landslide has been observed in the central part of the slope, mainly in quaternary clay and in its interface with sand clay and neogene clay. It is worth noticing that the value of the friction angle of the quaternary clay is much less than for the remaining materials. Numerical results presented below confirm the location of the landslide.

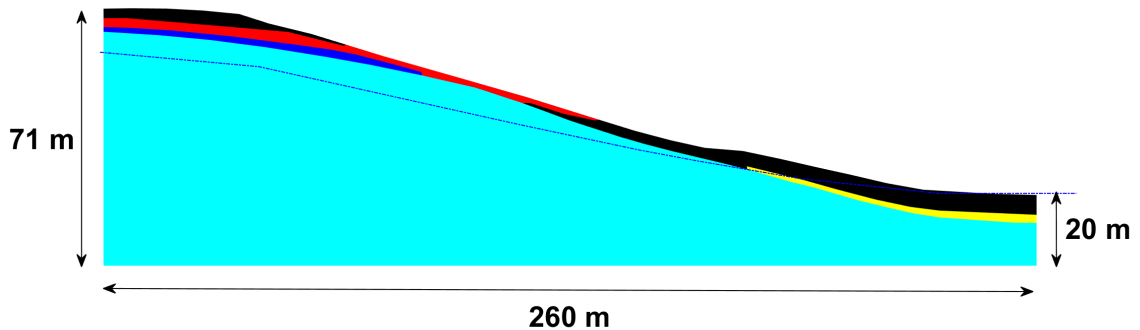


Figure 6: Geometry of the heterogeneous slope.

Computed safety factors for different approaches are listed in Table 3. We see that the safety factors are very close to 1 for all investigated approaches and thus the slope is unstable. The values received by the in-house Matlab codes are slightly lower than the remaining ones due to the usage of the local mesh adaptivity.

The initial mesh for computation in Comsol Multiphysics is depicted in Figure 7. This mesh reflects the material heterogeneity and has been also imported to Matlab. In Comsol Multiphysics, this mesh was then locally refined in the central part of the slope to achieve more accurate results. In Matlab, the original mesh was adaptively refined and 15 mesh levels were considered.

A detail of the finest Matlab mesh is depicted in Figure 8 together with the corresponding

Table 3: Safety factors for the heterogeneous slope and different approaches

	MATLAB	COMSOL	Plaxis
$\psi = \phi$ , assoc. model	1.05	1.09	1.08
$\psi = 0^\circ$ , Davis I	1.02	1.06	1.05
$\psi = 0^\circ$ , Davis II	1.02	1.06	—
$\psi = 0^\circ$ , current approach	—	—	1.06

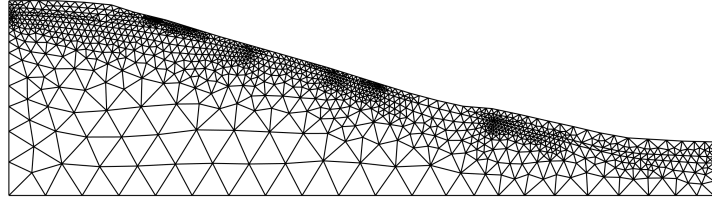


Figure 7: Initial mesh for the heterogeneous slope created in Comsol Multiphysics.

slip zone. For visualization of this zone, a norm of the deviatoric strain was used. The black curves in the figure depicts the material interface. We see that the zone is not too deep and its large part lies on the interface of the quaternary and neogene clays.

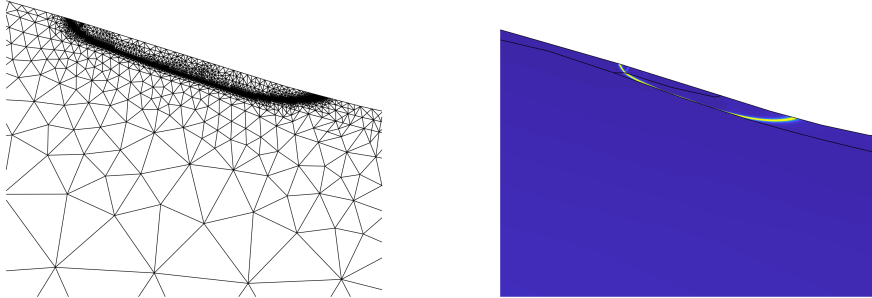


Figure 8: Detail of the finest mesh in Matlab and the corresponding slip zone on the material interface.

In Figure 9, we see the dependence of the safety factors on mesh adaptivity computed in Matlab for all three approaches. We observe that these curves are practically constant after a sufficiently large numbers of mesh refinements and thus the received values are almost independent of the mesh density. We also observe that the safety factor for the Davis I approach is slightly less than the one for Davis II. This is in accordance with our

theoretical results.

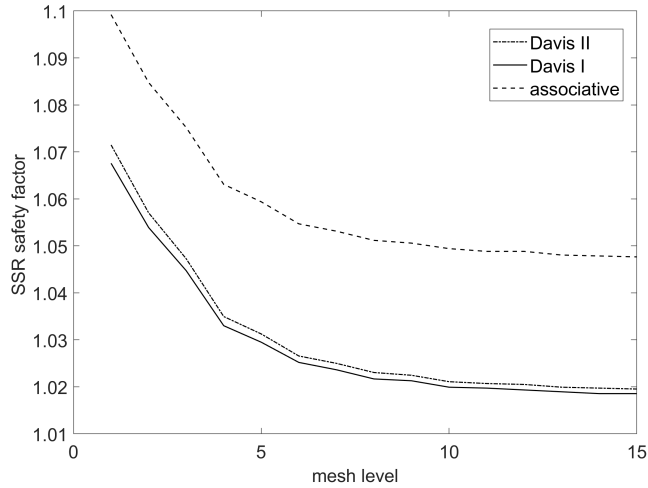


Figure 9: Safety factors for the homogeneous slope depending on mesh adaptivity.

## 8 Conclusion

This work has been inspired by recent ideas presented in [Tschuchnigg et al. (2015b)] where the shear strength reduction (SSR) method was interpreted as a parametrized limit analysis (LA) method. Based on these ideas, we have built in this paper a *rigorous* variant of the SSR method, analyzed and used it in geotechnics, independently of the LA method. The suggested variant is based on optimization problems, variational principles and on modifications of the Davis approach.

For numerical solution, a regularization method has been used and combined with the finite element and the damped Newton method. This solution concept leads to similar solvers which are standardly used in computational plasticity and thus it can be easily implemented within existing elastic-plastic codes. In particular, we have arised from our in-house Matlab codes [Cermak et al. (2019)] and completed them with local mesh adaptivity. Softwares Plaxis and Comsol Multiphysics have been used for comparison of the results. One of the presented numerical examples has followed from analysis of a real slope.

**Acknowledgment:** The authors acknowledge support for their work from the Czech Science Foundation (GAČR) through project No. 19-11441S. The authors also thank to

Dr. Alexej Kolcun for fruitful discussions on mesh adaptivity for regular and irregular meshes.

## 9 Appendix – closed form of the function $D_1$

For the sake of completeness, we introduce the closed form of the function

$$D_1(q(\lambda); \boldsymbol{\varepsilon}) = \sup_{\substack{\boldsymbol{\sigma} \in \mathbb{R}^{3 \times 3}_{sym} \\ \Phi(q(\lambda); \boldsymbol{\sigma}) \leq 0}} \left[ \boldsymbol{\sigma} : \boldsymbol{\varepsilon} - \frac{1}{2} \mathbb{C}^{-1} \boldsymbol{\sigma} : \boldsymbol{\sigma} \right]. \quad (9.1)$$

from Section 6. In literature (see, for example, [de Souza Neto et al. (2011), Sysala et al. (2017)]), one can find closed form of the derivative  $T_1$  of  $D_1$  representing the stress-strain relation but not  $D_1$ . Therefore, we try to fill this gap.

Beside  $\lambda \geq 0$ , this function also depends on the inelastic parameters  $c, \phi$  and the elastic parameters  $K, G$ . We construct the function  $D_1(q(\lambda); \boldsymbol{\varepsilon})$  only for such  $\lambda$  satisfying  $q(\lambda) = 1$ . For other choices of  $\lambda$ , it suffices to replace  $c$  and  $\phi$  with

$$c_{q(\lambda)} := \frac{c}{q(\lambda)}, \quad \phi_{q(\lambda)} := \arctan \frac{\tan \phi}{q(\lambda)}. \quad (9.2)$$

see also (2.13). To be in accordance with the derivation presented in [Sysala et al. (2017)], we shall write the yield criterion  $\Phi(1; \boldsymbol{\sigma}) \leq 0$  in the form

$$(1 + \sin \phi) \sigma_1 - (1 - \sin \phi) \sigma_3 - 2c \cos \phi \leq 0. \quad (9.3)$$

Next, we assume that the strain tensor  $\boldsymbol{\varepsilon}$  is given and its eigenvalues  $\varepsilon_1, \varepsilon_2, \varepsilon_3$  satisfy  $\varepsilon_1 \geq \varepsilon_2 \geq \varepsilon_3$ . Let  $\text{tr } \boldsymbol{\varepsilon} = \varepsilon_1 + \varepsilon_2 + \varepsilon_3$  denote the trace of  $\boldsymbol{\varepsilon}$  and  $\Lambda = \frac{1}{3}(3K - 2G)$  denote the first Lamé coefficient. As in the book [de Souza Neto et al. (2011)], we distinguish five possible cases: the elastic response, the return to the smooth portion of the Mohr-Coulomb pyramid, the return to the left edge, the return to the right edge, and the return to the apex of the pyramid.

**The elastic response.** This case happen if the elastic stress  $\mathbb{C}\boldsymbol{\varepsilon}$  satisfies  $\Phi(1; \mathbb{C}\boldsymbol{\varepsilon}) \leq 0$ , that is,

$$2\Lambda(\text{tr } \boldsymbol{\varepsilon}) \sin \phi + 2G(1 + \sin \phi)\varepsilon_1 - 2G(1 - \sin \phi)\varepsilon_3 - 2c \cos \phi \leq 0. \quad (9.4)$$

Then

$$D_1(1; \boldsymbol{\varepsilon}) = \frac{1}{2} \mathbb{C} \boldsymbol{\varepsilon} : \boldsymbol{\varepsilon} = \frac{1}{2} \Lambda (\text{tr } \boldsymbol{\varepsilon})^2 + G(\varepsilon_1^2 + \varepsilon_2^2 + \varepsilon_3^2). \quad (9.5)$$

If the criterion (9.4) does not hold then the plastic response occurs and we distinguish four possible cases of the return to the Mohr-Coulomb pyramid. We use the following auxiliary notation:

$$\begin{aligned} \gamma_{s,l} &= \frac{\varepsilon_1 - \varepsilon_2}{1 + \sin \phi}, & \gamma_{s,r} &= \frac{\varepsilon_2 - \varepsilon_3}{1 - \sin \phi}, \\ \gamma_{l,a} &= \frac{\varepsilon_1 + \varepsilon_2 - 2\varepsilon_3}{3 - \sin \phi}, & \gamma_{r,a} &= \frac{2\varepsilon_2 - \varepsilon_2 - \varepsilon_3}{3 + \sin \phi}. \end{aligned}$$

**The return to the smooth portion.** This case happen if (9.4) is not satisfied and

$$q_s(\boldsymbol{\varepsilon}) < S \min\{\gamma_{s,l}, \gamma_{s,r}\}, \quad (9.6)$$

where

$$q_s(\boldsymbol{\varepsilon}) = 2\Lambda(\text{tr } \boldsymbol{\varepsilon}) \sin \phi + 2G(1 + \sin \phi)\varepsilon_1 - 2G(1 - \sin \phi)\varepsilon_3 - 2c \cos \phi,$$

$$S = 4\Lambda \sin^2 \phi + 4G(1 + \sin^2 \phi).$$

Then,

$$D_1(1; \boldsymbol{\varepsilon}) = \frac{1}{2} \Lambda (\text{tr } \boldsymbol{\varepsilon})^2 + G(\varepsilon_1^2 + \varepsilon_2^2 + \varepsilon_3^2) - \frac{1}{2S} q_s^2(\boldsymbol{\varepsilon}). \quad (9.7)$$

**The return to the left edge.** This case happen if (9.4) is not satisfied and

$$\gamma_{s,l} < \gamma_{l,a}, \quad L\gamma_{s,l} \leq q_l(\boldsymbol{\varepsilon}) < L\gamma_{l,a}, \quad (9.8)$$

where

$$q_l(\boldsymbol{\varepsilon}) = 2\Lambda(\text{tr } \boldsymbol{\varepsilon}) \sin \phi + G(1 + \sin \phi)(\varepsilon_1 + \varepsilon_2) - 2G(1 - \sin \phi)\varepsilon_3 - 2c \cos \phi,$$

$$L = 4\Lambda \sin^2 \phi + G(1 + \sin \phi)^2 + 2G(1 - \sin \phi)^2.$$

Then,

$$D_1(1; \boldsymbol{\varepsilon}) = \frac{1}{2} \Lambda (\text{tr } \boldsymbol{\varepsilon})^2 + G\left[\frac{1}{2}(\varepsilon_1 + \varepsilon_2)^2 + \varepsilon_3^2\right] - \frac{1}{2L} q_l^2(\boldsymbol{\varepsilon}). \quad (9.9)$$

**The return to the right edge.** This case happen if (9.4) is not satisfied and

$$\gamma_{s,r} < \gamma_{r,a}, \quad R\gamma_{s,r} \leq q_r(\boldsymbol{\varepsilon}) < R\gamma_{r,a}, \quad (9.10)$$

where

$$q_r(\boldsymbol{\varepsilon}) = 2\Lambda(\text{tr } \boldsymbol{\varepsilon}) \sin \phi + 2G(1 + \sin \phi)\varepsilon_1 - G(1 - \sin \phi)(\varepsilon_2 + \varepsilon_3) - 2c \cos \phi,$$

$$R = 4\Lambda \sin^2 \phi + 2G(1 + \sin \phi)^2 + G(1 - \sin \phi)^2.$$

Then,

$$D_1(1; \boldsymbol{\varepsilon}) = \frac{1}{2}\Lambda(\text{tr } \boldsymbol{\varepsilon})^2 + G\left[\varepsilon_1^2 + \frac{1}{2}(\varepsilon_2 + \varepsilon_3)^2\right] - \frac{1}{2R}q_r^2(\boldsymbol{\varepsilon}). \quad (9.11)$$

**The return to the apex.** This case happen if (9.4) is not satisfied and

$$q_a(\boldsymbol{\varepsilon}) \geq A \max\{\gamma_{l,a}, \gamma_{r,a}\}, \quad (9.12)$$

where

$$q_a(\boldsymbol{\varepsilon}) = 2K(\text{tr } \boldsymbol{\varepsilon}) \sin \phi - 2c \cos \phi, \quad A = 4K \sin^2 \phi.$$

Then,

$$D_1(1; \boldsymbol{\varepsilon}) = \frac{1}{2}K(\text{tr } \boldsymbol{\varepsilon})^2 - \frac{1}{2A}q_a^2(\boldsymbol{\varepsilon}) = \frac{c}{\tan \phi}(\text{tr } \boldsymbol{\varepsilon}) - \frac{c^2}{2K \tan^2 \phi}. \quad (9.13)$$

## References

[Brinkgreve and Bakker (1991)] Brinkgreve, R. B. J. & Bakker, H. L. (1991). Non-linear finite element analysis of safety factors. Proceedings of the international conference on computer methods and advances in geomechanics, pp. 1117–1122. Rotterdam, the Netherlands: Balkema.

[Brinkgreve (2011)] Brinkgreve, R. B. J., Swolfs, W. M. & Engin, E. (2011). Plaxis 2D 2011 – user manual. Delft, the Netherlands: Plaxis bv.

[Cermak et al. (2015)] Cermak, M., Haslinger, J., Kozubek, T., Sysala, S. (2015). Discretization and numerical realization of contact problems for elastic-perfectly plastic bodies. PART II–numerical realization, limit analysis. *ZAMM-Journal of Applied Mathematics and Mechanics/Zeitschrift für Angewandte Mathematik und Mechanik*, 95(12), 1348–1371.

[Cermak et al. (2018)] Čermák, M., Sysala, S., & Valdman, J. (2018). MATLAB FEM package for elastoplasticity, [https://github.com/matlabfem/matlab\\_fem\\_elastoplasticity](https://github.com/matlabfem/matlab_fem_elastoplasticity).

[Cermak et al. (2019)] Čermák, M., Sysala, S., & Valdman, J. (2019). Efficient and flexible MATLAB implementation of 2D and 3D elastoplastic problems. *Applied Mathematics and Computation*, 355, 595–614.

[Chen and Liu (1990)] Chen, W. and Liu, X.L. (1990). *Limit Analysis in Soil Mechanics*. Elsevier.

[Christiansen (1990)] Christiansen, E. (1996). *Limit analysis of collapse states*. In P. G. Ciarlet and J. L. Lions, editors, *Handbook of Numerical Analysis*, Vol IV, Part 2, North-Holland, 195–312.

[Davis (1968)] Davis, E. H. (1968). Theories of plasticity and failure of soil masses. In *Soil mechanics: selected topics* (ed. I. K. Lee), pp. 341–354. New York, NY, USA: Elsevier.

[Dawson et al. (1999)] Dawson, E. M., Roth, W. H. & Drescher, A. A. (1999). Slope stability analysis by strength reduction. *Géotechnique* 49, No. 6, 835–840, <http://dx.doi.org/10.1680/geot.1999.49.6.835>.

[Duncan (1996)] Duncan, J. M. (1996). State of the art: limit equilibrium and finite-element analysis of slopes. *Journal of Geotechnical engineering*, 122(7), 577–596.

[de Souza Neto et al. (2011)] de Souza Neto, E. A., Peric, D., & Owen, D. R. (2011). Computational methods for plasticity: theory and applications. John Wiley & Sons.

[Ekeland and Temam (1974)] Ekeland, I. and Temam, R. (1974). *Analyse Convexe et Problèmes Variationnels*. Dunod, Gauthier Villars, Paris.

[Griffiths and Lane (1999)] Griffiths, D. V. & Lane, P. A. (1999). Slope stability analysis by finite elements. *Géotechnique* 49, No. 3, 387–403, <http://dx.doi.org/10.1680/geot.1999.49.3.387>.

[Hamlaoui et al. (2017)] Hamlaoui, M., Oueslati, A., & De Saxcé, G. (2017). A bipotential approach for plastic limit loads of strip footings with non-associated materials. *International Journal of Non-Linear Mechanics*, 90, 1–10.

[Han and Reddy (2012)] Han, W., & Reddy, B. D. (2012). Plasticity: mathematical theory and numerical analysis (Vol. 9). Springer Science & Business Media.

[Haslinger et al. (2016a)] Haslinger, J., Repin, S., Sysala, S. (2016). A reliable incremental method of computing the limit load in deformation plasticity based on compliance: Continuous and discrete setting. *Journal of Computational and Applied Mathematics* 303, 156–170.

[Haslinger et al. (2016b)] Haslinger, J., Repin, S., Sysala, S (2016). Guaranteed and computable bounds of the limit load for variational problems with linear growth energy functionals. *Applications of Mathematics* 61, 527–564.

[Haslinger et al. (2019)] Haslinger, J., Repin, S., Sysala, S. (2019). Inf-sup conditions on convex cones and applications to limit load analysis. *Mathematics and Mechanics of Solids* 24, 3331–3353.

[Hjiaj et al. (2003)] Hjiaj, M., Fortin, J., & de Saxcé, G. (2003). A complete stress update algorithm for the non-associated Drucker–Prager model including treatment of the apex. *International Journal of Engineering Science*, 41(10), 1109–1143.

[Krabbenhoft (2012)] Krabbenhoft, K., Karim, M. R., Lyamin, A. V., & Sloan, S. W. (2012). Associated computational plasticity schemes for nonassociated frictional materials. *International Journal for Numerical Methods in Engineering*, 90(9), 1089–1117.

[Reddy and Sysala (2020)] Reddy, B.D. & Sysala, S. (2020). Bounds on the elastic threshold for problems of dissipative strain-gradient plasticity. *Journal of the Mechanics and Physics of Solids* 143, 104089.

[Repin et al. (2018)] Repin, S., Sysala, S., Haslinger, J. Computable majorants of the limit load in Hencky’s plasticity problems. *Comp. & Math. with Appl.* (2018) 75: 199–217.

[Sloan (2013)] Sloan SW (2013). Geotechnical stability analysis, *Géotechnique*, 63, 531–572.

[Sysala (2012)] Sysala, S. (2012). Application of a modified semismooth Newton method to some elasto-plastic problems. *Mathematics and Computers in Simulation*, 82(10), 2004–2021.

[Sysala (2014)] Sysala, S. (2014). Properties and simplifications of constitutive time-discretized elastoplastic operators. *ZAMM-Journal of Applied Mathematics and Mechanics/Zeitschrift für Angewandte Mathematik und Mechanik*, 94(3), 233–255.

[Sysala et al. (2019)] Sysala, S., Blaheta, R., Kolcun, A., Ščučka, J., Souček, K., & Pan, P. Z. (2019). Computation of Composite Strengths by Limit Analysis. *Key Engineering Materials*, 810, 137–142.

[Sysala et al. (2017)] Sysala, S., Čermák, M., & Ligurský, T. (2017). Subdifferential-based implicit return-mapping operators in Mohr-Coulomb plasticity. *ZAMM-Journal of Applied Mathematics and Mechanics/Zeitschrift für Angewandte Mathematik und Mechanik*, 97(12), 1502–1523.

[Sysala et al. (2015)] Sysala, S., Haslinger, J., Hlaváček, I., Cermak, M. (2015). Discretization and numerical realization of contact problems for elastic-perfectly plastic bodies. PART I–discretization, limit analysis. *ZAMM-Journal of Applied Mathematics and Mechanics/Zeitschrift für Angewandte Mathematik und Mechanik*, 95(4), 333–353.

[Sysala et al. (2016)] Sysala, S., Cermak, M., Koudelka, T., Kruis, J., Zeman, J., & Blaheta, R. (2016). Subdifferential-based implicit return-mapping operators in computational plasticity. *ZAMM-Journal of Applied Mathematics and Mechanics/Zeitschrift für Angewandte Mathematik und Mechanik*, 96(11), 1318–1338.

[Temam (1985)] Temam, R. (1985). *Mathematical Problems in Plasticity*. Gauthier-Villars, Paris.

[Tschuchnigg et al. (2015a)] Tschuchnigg, F., Schweiger, H.F., Sloan, S.W., Lyamin, A.V., & Raissakis, I. (2015). Comparison of finite-element limit analysis and strength reduction techniques. *Géotechnique*, 65(4), 249–257.

[Tschuchnigg et al. (2015b)] Tschuchnigg, F., Schweiger, H.F., & Sloan, S.W. (2015). Slope stability analysis by means of finite element limit analysis and finite element strength reduction techniques. Part I: Numerical studies considering non-associated plasticity. *Computers and geotechnics*, 70, 169–177.

[Tschuchnigg et al. (2015c)] Tschuchnigg, F., Schweiger, H.F., & Sloan, S.W. (2015). Slope stability analysis by means of finite element limit analysis and finite element strength reduction techniques. Part II: Back analyses of a case history. *Computers and geotechnics*, 70, 178–189.

[Yu (2006)] Yu, H.-S. (2006). *Plasticity and Geotechnics*, Springer Science+Business Media, New York.

[Zienkiewicz et al. (1975)] Zienkiewicz, O.C., Humpheson, C., and Lewis, R.W. (1975). Associated and non-associated visco-plasticity and plasticity in soil mechanics. *Géotechnique*, 25(4), 671–689.